Article

Applied Spectroscopy

Applied Spectroscopy
0(0) 1–10

DOI: 10.1177/0003702816645605
asp.sagepub.com
SAGE

Screening of Astaxanthin-Hyperproducing *Haematococcus pluvialis* Using Fourier Transform Infrared (FT-IR) and Raman Microspectroscopy

Jinghua Liu[1,2] and Qing Huang[1,2,3]

Abstract

Haematococcus pluvialis has promising applications owing to its ability to accumulate astaxanthin under stress conditions. In order to acquire higher astaxanthin productivity from *H. pluvialis*, it is critical not only to develop efficient mutagenesis techniques, but also to establish rapid and effective screening methods which are highly demanded in current research and application practice. In this work, we therefore attempted to develop a new approach to screening the astaxanthin-hyperproducing strains based on spectroscopic tools. Using Fourier transform infrared (FT-IR) and Raman microspectroscopy, we have achieved rapid and quantitative analysis of the algal cells in terms of astaxanthin, β-carotene, proteins, lipids, and carbohydrates. In particular, we have found that the ratio of the IR absorption band at 1740 cm^{-1} to the band at 1156 cm^{-1} can be utilized for identifying astaxanthin-hyperproducing strains. This work may therefore open a new avenue for developing high-throughput screening methods necessary for the microbial mutant breeding industry.

Keywords

Astaxanthin, FT-IR microspectroscopy, *haematococcus pluvialis*, raman microspectroscopy

Date received: 1 October 2015; accepted: 17 January 2016

Introduction

Astaxanthin (3,3′-dihydroxy-β,β′-carotene-4,4′-dione) is a kind of carotenoid pigment that is well known for its higher activity to scavenge reactive oxygen species (ROS) than many other natural antioxidants.[1,2] Being a potent biological antioxidant, it has not only become a rich pigment source in aquaculture, but has also shown potential application in the pharmaceutical and cosmetic industries.[3,4] Especially in recent years, the demand for astaxanthin has surged in the nutraceutical market due to its potential human health benefits such as cardiovascular disease prevention, promotion of the immune response, immune system boosting, UV-light protection, cataract prevention, etc.[5]

However, astaxanthin must be obtained from the diet because it cannot be synthesized by animals and humans themselves. Natural astaxanthin can be obtained from the unicellular freshwater green microalga *Haematococcus pluvialis*, which can accumulate astaxanthin under stress conditions such as nutrient deprivation, increased salinity, acetate addition, high/low temperature, high irradiance, etc.[6,7] Yet the industrial large-scale production of *H. pluvialis* is still a challenging task because of the intrinsic shortcomings of natural *H. pluvialis*, such as slow growth rate, susceptibility to contamination, and low biomass concentration.[8] Researchers have been striving to improve astaxanthin production in *H. pluvialis* mutants through varied approaches, including chemical, physical, and biological mutagenesis methods.[9–11] In the meantime, in order to improve the effectiveness of breeding of astaxanthin-hyperproducing mutants of *H. pluvialis*, it is also critical to develop effective tools for screening of astaxanthin-hyperproducing strains quickly and conveniently. Traditionally, the screening process is performed by

[1]Institute of Technical Biology and Agriculture Engineering, Hefei Institutes of Physical Science, Key Lab of Ion-Beam Bioengineering, Chinese Academy of Sciences, Hefei, China
[2]School of Life Science, University of Science and Technology of China, Hefei, China
[3]School of Nuclear Science and Technology, University of Science and Technology of China, Hefei, China

Corresponding author:
Qing Huang, Key Lab of Ion-Beam Bioengineering, Chinese Academy of Sciences, P.O. Box 1138, Hefei 230031, China.
Email: huangq@ipp.ac.cn

plating the mutated population of microalgal cells onto agar to form colonies, and then the colonies are picked out from the agar followed by cultivation in Erlenmeyer flasks with liquid media for biochemical assays on growth rate, photosynthetic activity, pigment content, gene expression, etc. For example, Chumpolkulwong et al. used biochemical assay for astaxanthin evaluation to screen compacting-resistant *H. pluvialis* mutants of high growth rate and astaxanthin productivity.[12] Kamath et al. distinguished the astaxanthin hyper-producing mutants by identifying the high transcript level of carotenoid biosynthetic genes.[10] However, these traditional methods are generally time-consuming, requiring expensive instruments and sophisticated operations.[13] So it still remains a big challenge for researchers to explore more effective high-throughput screening methods for astaxanthin hyper-producing mutants.

Encouragingly, nowadays spectroscopic tools such as Fourier transform infrared (FT-IR) and Raman spectroscopy techniques have emerged as promising tools for high-throughput screening applications because they can be utilized to distinguish and quantify various vital components such as proteins, lipids, nucleic acids, and carbohydrates in biological systems; moreover, they have the advantages of simple, fast, non-invasive, and multiplex measurements.[14] In fact, the application of FT-IR and Raman spectroscopy in studying and screening microorganisms has now attracted increasing attention. For instance, Meanwell and Shama utilized FT-IR spectroscopy for isolation of streptomycin hyper-producing mutants on agar.[15] Li et al. and Sayin et al. both screened different yeast species by surface-enhanced Raman spectroscopy.[16,17] Helm et al. employed FT-IR spectroscopy to detect intracellular components such as granules, capsules, and endospores in intact bacteria.[18] Moreover, with the development of microscopic imaging technology, there is also a new trend to integrate advanced spectrometers with high-resolution microscopes, so the technique termed as "microspectroscopy" of FT-IR or Raman has now become more and more popular, especially for spatially-resolved and real-time *in situ* measurements of biological systems at the cellular or even subcellular level.[19–24] In addition, other techniques such as coherent anti-Stokes Raman scattering (CARS) microscopy have also been employed in rapid cell-imaging due to their advantages in terms of high sensitivity, chemical specificity, and rapid non-destructive screening; in particular, it has been reported that CARS was used in the study of carotenoids in microalgae.[25–27]

In this context, therefore, we initiated the application of FT-IR and Raman microspectroscopy in the study of different *H. pluvialis* strains, and attempted to establish a new method based on the spectroscopic approach that can facilitate the astaxanthin hyper-producing alga screening process. As a result, by making use of the tools of FT-IR and Raman microspectroscopy, and with the assistance of the chemometrics approach, such as principal component analysis (PCA) and multivariate curve resolution (MCR) algorithms, we were able to analyze different algal strains and identify the astaxanthin hyper-producing strains. It was demonstrated that the combination of FT-IR and Raman microspectroscopy could be very useful in the screening of astaxanthin-hyperproducing algal strains.

Experimental Procedures

Algal Culture and Growth Conditions

The wild-type (WT) *H. pluvialis* (strain FACHB-712) was obtained from the Freshwater Algae Culture Collection of the Chinese Academy of Sciences. The different algal mutant strains, namely, M3, M14, M16, M20, M29, and M33, were obtained in our own lab by treating the WT strain with plasma irradiation. All the samples were inoculated into 250 mL Erlenmeyer flasks and cultivated in a Bold's Basal Medium,[28] under a cycle of 12 h light/12 h dark illumination conditions at $25 \pm 0.5^{\circ}$C with low light intensity of 50 μmol photons m^{-2} s^{-1} or high light intensity of 150 μmol photons m^{-2} s^{-1}, for astaxanthin accumulation during 5, 10, 20, 30, 40, and 50 days according to the protocol reported previously.[29]

Extraction and Analysis of Astaxanthin

The high growth rate mutants were treated with a solution of 5% KOH in 30% methanol to destroy the chlorophyll and then the cells were harvested by centrifugation. The cells were then broken by grinding with a homogenizer and then the astaxanthin was extracted with DMSO at 70°C until the cell debris was totally white. The absorbance of the extracts was determined at the wavelength of 492 nm and the amount of astaxanthin was calculated according to the methods proposed by Davies,[30] and by Boussiba and Vonshak.[31]

Measurements via FT-IR and Raman Microspectroscopy

Once the *H. pluvialis* cells grew sufficiently, 50 μL washed samples were dropped on BaF_2 substrates dried at 40°C for 3 h for FT-IR measurements and on quartz substrates for Raman measurements. For the single-cell measurements via FT-IR and Raman microspectroscopy, five single cells were selected randomly as being representative for inspection.

The FT-IR measurements were performed at the National Synchrotron Radiation Laboratory (NSRL, China) using a synchrotron FT-IR spectrometer (Bruker IFS 66v/s) which was coupled with an IR microscope (Hyperion 3000). The spectra were recorded in transmission mode with 4 cm^{-1} resolution, encompassing the mid-IR region from 4000 cm^{-1} to 900 cm^{-1}, with 256 scans and 2 min or 512 scans and 4 min for each single-spot FT-IR spectrum. The spatial resolution was 6 μm × 6 μm for infrared imaging.

The Raman spectra were recorded by a Raman microspectrometer (XploRA, Horiba Jobin Yvon) equipped with a 532 nm laser and an Olympus 50 × long working distance lens. The power density measured at the sample was less than 1 mW. Spectral images were obtained by raster scanning using 1 μm × 1 μm steps. Images of a cell were acquired using the 1 s integration for each single-spot Raman spectrum. The time to acquire an image depended on the sample size, and for the Raman image containing 300 spectra (spots), the recording time was typically about 10 min.

Multivariate Statistical Analysis

The raw FT-IR spectra were baseline-corrected and vector normalized before being converted to second derivatives using the OPUS software provided by Bruker. The PCA was conducted based on the second derivative of the FT-IR spectra. The Raman spectra were analyzed using MCR.[32,33] The MCR software packages were available online from Eigenvector Research Inc., and the MCR treatment could lead to separate spectra for pure chemical components and relative concentration maps for each component.[34]

Results and Discussion

Biochemical Assay of Algal Strains

Before evaluation via FT-IR spectroscopy, the production of astaxanthin was at first measured via biochemical assay. To stimulate and accelerate the massive production of astaxanthin, high light irradiation was employed which can induce morphological change from vegetative cells to cysts with the concomitant accumulation of astaxanthin.[31] The algal strains were cultured under high light irradiation with intensity of 150 μmol photons $m^{-2} s^{-1}$. The production of astaxanthin reached a maximal and constant level after 20–30 days of high light irradiation (here we only present the data obtained from algae cultured for 20 days). Figure 1 shows the results of astaxanthin in wild-type and other different mutant strains, namely, M3, M14, M16, M20, M29, and M33. Compared to the WT strain, the astaxanthin in M3 (3.35% w/w) is 1.59-fold higher than the WT strain (2.11% w/w). Vidhyavathi et al. and Kamath et al. reported that they obtained astaxanthin hyper-producing strains with 2.45% w/w and 3.95% w/w for the astaxanthin production.[10,35] So in our case, M3 could also be regarded as the astaxanthin hyper-producing strain in this work.

Analysis Using FT-IR Microspectroscopy and Imaging

The above biochemical assay showed that different colonies had different abilities for astaxanthin production. In principle, the chemicals can also be analyzed through spectroscopic methods because they can provide unique fingerprints of the chemicals, and, moreover, they have the advantages in non-invasive rapid and effective high-throughput screening measurements. For example, it has been reported that FT-IR microspectroscopy and imaging can reveal the biochemical changes of the microorganisms even without obvious physiological and morphological effects.[20] Therefore, in this work we tried using FT-IR microspectroscopy to make the evaluation of chemical contents in different algal strains. Figure 2 shows the photomicrographs and the chemical images of the different *H. pluvialis* mutants under high light irradiation condition for 20 days. Figure 2b shows the typical FT-IR spectrum recorded for obtaining the FT-IR images in Figure 2a. It should be noted that the astaxanthin was evaluated after algal growth for 20 days because the cell numbers and astaxanthin formation and accumulation reached almost maximum after 20 days (see Supplemental Figure 1 online). During the growth stages of *H. pluvialis*, it has both motile and non-motile forms. The proliferation of *H. pluvialis* cells is fast under favorable conditions; however, once the growing conditions become unfavorable, such as high light irradiance, the cells increase their volume drastically and enter a resting stage in which the cells accumulate astaxanthin.[6] Although there was variability in cellular astaxanthin production from cell to cell (so the production of astaxanthin in *H. pluvialis* has been presented by the unit pg/cell),[31] the overall content of astaxanthin remained high and steady after the *H. pluvialis* cells were exposed to high light for 20–30 days.

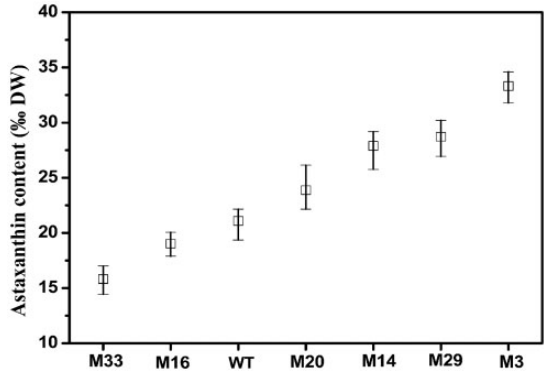

Figure 1. Total astaxanthin accumulation of various *H. pluvialis* strains. The mean values with minimum and maximum are shown.

Figure 2a also shows that the *H. pluvialis* cells have similar appearance but different concentration distributions for chemical components such as β-carotene, astaxanthin, proteins, lipids, and carbohydrates. Compared with the WT strain, the FT-IR signals of β-carotene, astaxanthin, proteins, lipids, and carbohydrates are relatively higher in M3 strain. It has been reported that β-carotene is the precursor for astaxanthin and located in chloroplast where it is

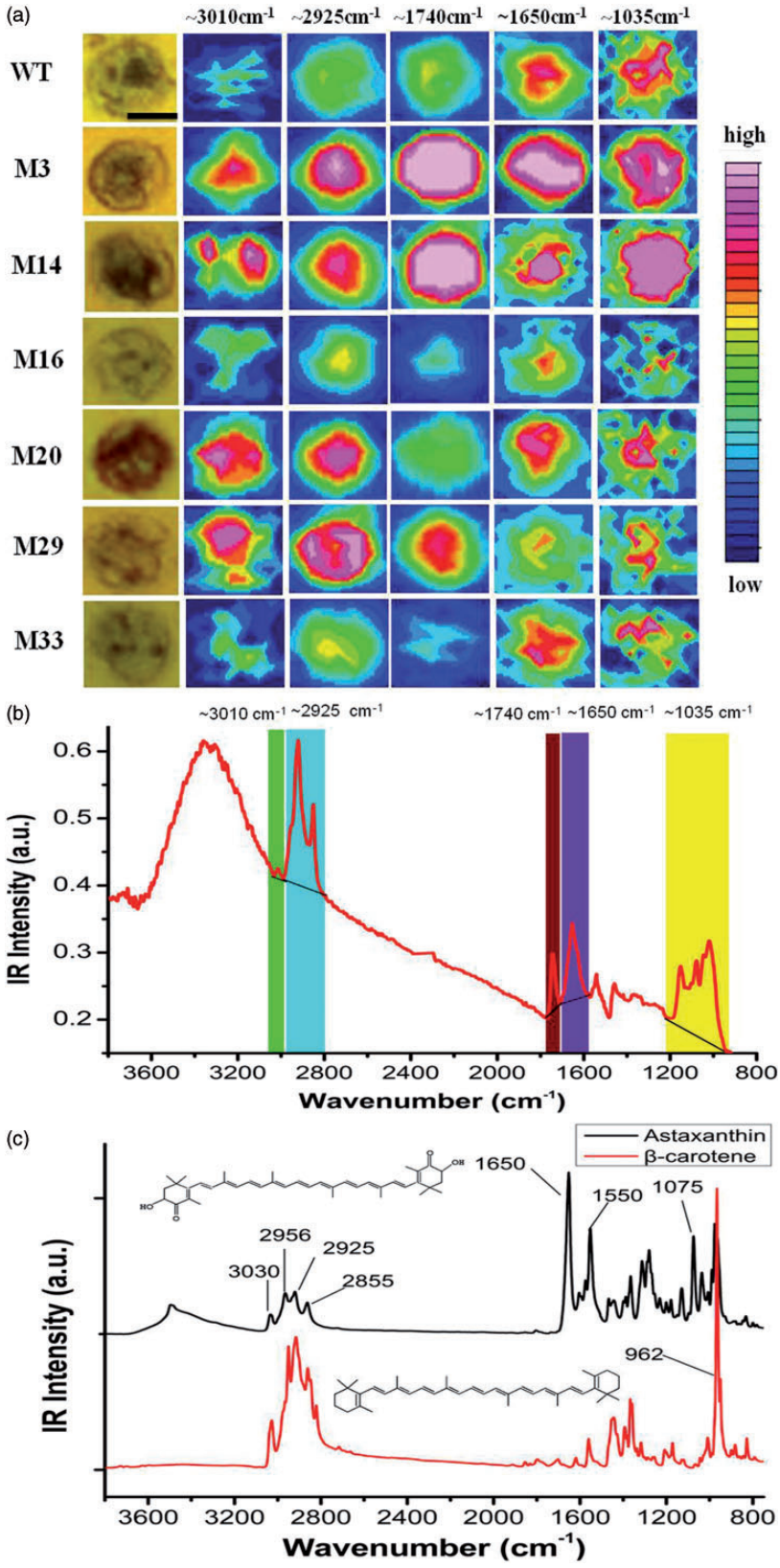

Figure 2. Photomicrographs and FT-IR mappings for different *H. pluvialis* strains (scale bar is 20 μm). (a) Chemical mappings for different components in the algal cell: map for C=C at the absorption band around 3010 cm^{-1}; map for lipids at stretching of CH_3 and CH_2 around 2925 cm^{-1}; map for C=O at the absorption band around 1740 cm^{-1}; map for proteins at stretching of Amide I around 1650 cm^{-1}; map for carbohydrates at the absorption band around 1035 cm^{-1} (b) The selected peaks for the spectroscopic images. (c) The FTIR spectra of pure astaxanthin and β-carotene.

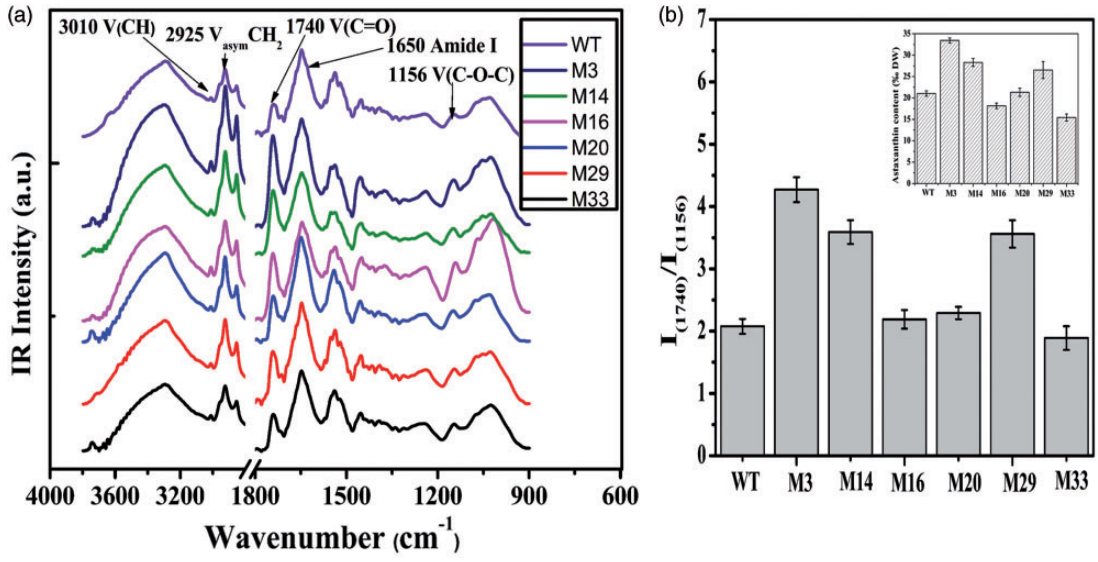

Figure 3. FT-IR spectra of wild and astaxanthin-hyperproducing *H. pluvialis* strains (a) and the analysis of the FT-IR absorbance band area ratio *I*(1740)/*I*(1156) for different strains (b). Error bars are calculated from three independent repetitions.

transported towards the cytoplasmic lipid vesicles via carotenoid-binding proteins before it is converted into astaxanthin.[36] On the other hand, the cell wall of *H. pluvialis* is composed of a complex matrix of carbohydrate, proteins, and other compounds. As the cell transforms from a green motile flagellate to a non-motile green cell and then to a red cyst accompanied by massive accumulation of astaxanthin and expansion of cell volume, the cell wall undergoes continuous, dynamic modifications from a primary cell wall eventually to a thick secondary cell wall.[37] Therefore, it can be inferred that the higher levels of β-carotene, lipid, and carbohydrate just reflect the transformation of cell stages and accumulation of astaxanthin in *H. pluvialis* (see Supplemental Figure 2 online).

It should be noted that the high content of β-carotene and low level of astaxanthin in M29 and M20 strains were detected by FT-IR microspectroscopy during 20 days under high light stress, while the high content of astaxanthin in *H. pluvialis* after light stress for 30 days was detected by biochemical assay, as shown in Figure 1. This means that with prolonged growth time, more β-carotene in these strains was transformed to astaxanthin.

Figure 3 shows the FT-IR spectra of the algal cells and the corresponding spectral analysis. The IR-band at 3010 cm^{-1} is assigned to the vibrations of CH=CH in carotenoids (both β-carotene and astaxanthin).[38] The bands at 2925 and 2855 cm^{-1} are assigned to the antisymmetric and symmetric C–H stretch from CH_2 groups in lipid and this group is also contained in the carbon ring structure of astaxanthin (shown in Figure 2c). The band at 1740 cm^{-1} is attributed to the vibrations of C=O in lipids. It should be noted that the lower frequency at 1650 cm^{-1} can be found in the FT-IR spectrum of pure astaxanthin, as shown in Figure 2c, which maybe come from the C=O group in astaxanthin due to its conjugation to a C=C group.[39] Thus, the whole IR band at 1650 cm^{-1} can be assigned to the Amide I of proteins and the C=O band of astaxanthin. The band at 1156 cm^{-1} is dominated by C–O–C in carbohydrate.[40] Interestingly, from the spectral analysis we found that the ratio of the absorption C=O at 1740 cm^{-1} to C–O–C at 1156 cm^{-1} (Figure 3b) is concomitant with the astaxanthin level, as evaluated by the biochemical assay shown in Figure 1. This is understandable because the FT-IR absorption band at 1156 cm^{-1} attributed to C–O–C for carbohydrate can be used as an internal standard (the composition of *H. pluvialis* algae normally consists of carotenoid, fatty acid, protein, and carbohydrate, and the proportion of carbohydrates in *H. pluvialis* maintains a high level and it can reflect the biomass in algal strains),[41] while the infrared band at 1740 cm^{-1} is mainly attributed to C=O of lipid, and lipid is just closely related to the content of astaxanthin, as it has been reported that the accumulation of lipids is mainly in triacylglycerols and is linearly correlated with the accumulation of astaxanthin.[42] Under stress conditions, the astaxanthin is accumulated, monoesterified, and stored in cytoplasmic lipid bodies. In fact, we also confirmed this by using the Nile red fluorescence method for quantitative measurement of neutral lipids of *H. pluvialis* at different stages (see Supplemental Figure 4 online), which confirms that high content of lipid is related to high content of astaxanthin production in the algal cells.

Moreover, we also observed that the concentration and distribution of the cellular components changed with culture time in the *H. pluvialis* cells (see Supplemental Figure 2 online). Under light-stress condition, the biomass composition was significantly changed, and the

accumulation of astaxanthin was accompanied by the decrease of β-carotene and the increase of the carbohydrate and lipid. The FT-IR imaging thus indicates that the fast increase in protein and lipid may be related to carotenogenesis enzymes and cytoplasmic lipid vesicles which play a crucial role in the carotenoid transformation and biosynthetic pathway of the *H. pluvialis*.[43] For example, in M3 strain, the fast increase of polysaccharides was observed to be coinciding with massive accumulation of astaxanthin and expansion of cell volume.

Therefore, although there might be other precursors for astaxanthin between β-carotene and astaxanthin, such as canthaxanthin, and many genes related to the enzymes for astaxanthin synthesis, it turned out that the astaxanthin hyper-producing strains obtained in this work were mainly dependent on the precursor of β-carotene. For the mutation experiment, we actually also obtained many other mutants (see Supplementary Table 1 online) which however did not give rise to higher production of astaxanthin. The astaxanthin contents of these strains were measured, and the ratios of *I*(1740)/*I*(1156) were evaluated with the results listed in Supplementary Table 1. In comparison with the biochemical assay result, we found that the evaluation based on the IR band ratio of *I*(1740)/*I*(1156) appears fairly good in evaluation and prediction of astaxanthin content in the algal strains. Within the reasonable error (say 15% of absolute error for evaluation of astaxanthin content), the screening accuracy based on the ratio of *I*(1740)/*I*(1156) can be higher over 80%. Therefore, we recommend that this spectral intensity ratio can be utilized as an empirical parameter for identifying the high astaxanthin-yield strains.

In addition, we also examined other infrared absorption band ratios, which are however less indicative for astaxanthin production in *H. pluvialis* (see Supplemental Figure 3 online). For example, the ratio of the absorption peak at 1650 cm^{-1} to C–O–C at 1156 cm^{-1} is not well concomitant with the astaxanthin level because the intensity of this band arising from proteins inside the cells as well as astaxanthin.

Analysis via Raman Microspectroscopy and Imaging

In parallel, Raman microspectroscopy was also employed for the algal cell analysis. Under the condition of 20 days of high light irradiation, the vegetable cells transformed into cysts, and the resulting spectral images of different mutants are shown in Figure 4. The spectrum of astaxanthin shows two prominent characteristic bands at 1516 cm^{-1} and 1157 cm^{-1} which are assigned to C=C and C–C stretching vibrations of the chain bonds, respectively.[44] The Raman spectrum of β-carotene is similar to the Raman spectrum of astaxanthin but there are slight shifts for the C=C and C–C bands (Figure 4b) For distinguishing the different components, a special and very useful processing method,

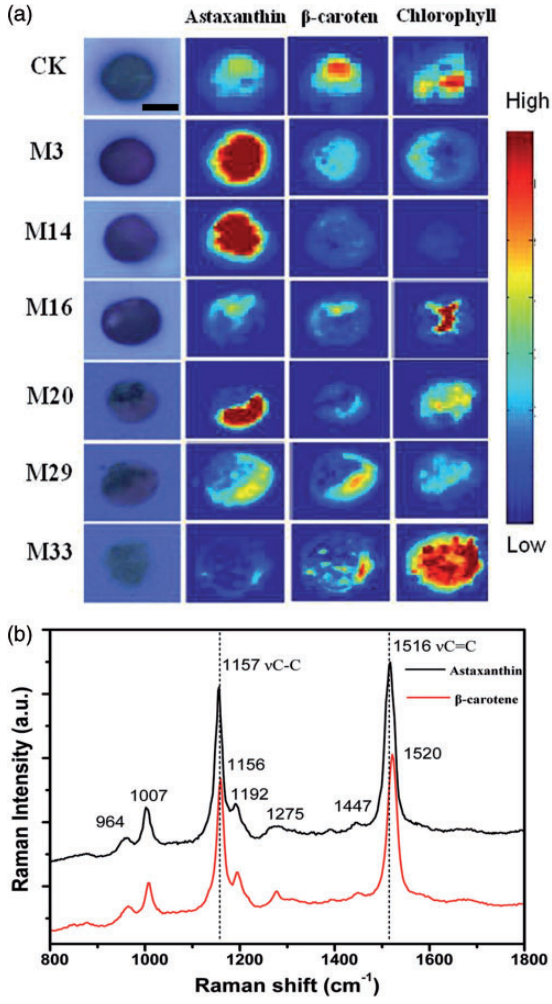

Figure 4. (a) The Raman MCR maps for components representing chlorophyll, astaxanthin, and β-carotene in different strains (scale bar is 20 μm) cultured for 20 days. (b) The Raman spectra of pure astaxanthin and β-carotene for reference.

namely, the MCR algorithm, was applied in the spectral analysis, so that the independently varying spectra of different components could be extracted from highly overlapping Raman spectral data.[34] In principle, the MCR analysis can resolve mixtures without requiring pure component training spectra, so it has versatile applications in spectroscopy, multi-fluorophore fluorescence imaging, spontaneous Raman imaging, and photoacoustic imaging.[45] But MCR has a limitation if there is some intensity ambiguity, so it requires good chemical contrast in the examined samples.[46] In our case for the MCR treatment, the fluorescence bands originated from cellular autofluorescence and fluorescence emission attributed to chlorophyll can be extracted (the representative spectra of astaxanthin, β-carotene, and chlorophyll are present in Supplemental Figure 5 online). Therefore, although the carotenoids and lipids have almost the same bands in the region 800–1800 cm^{-1}, and so cannot be distinguished from each other in the original

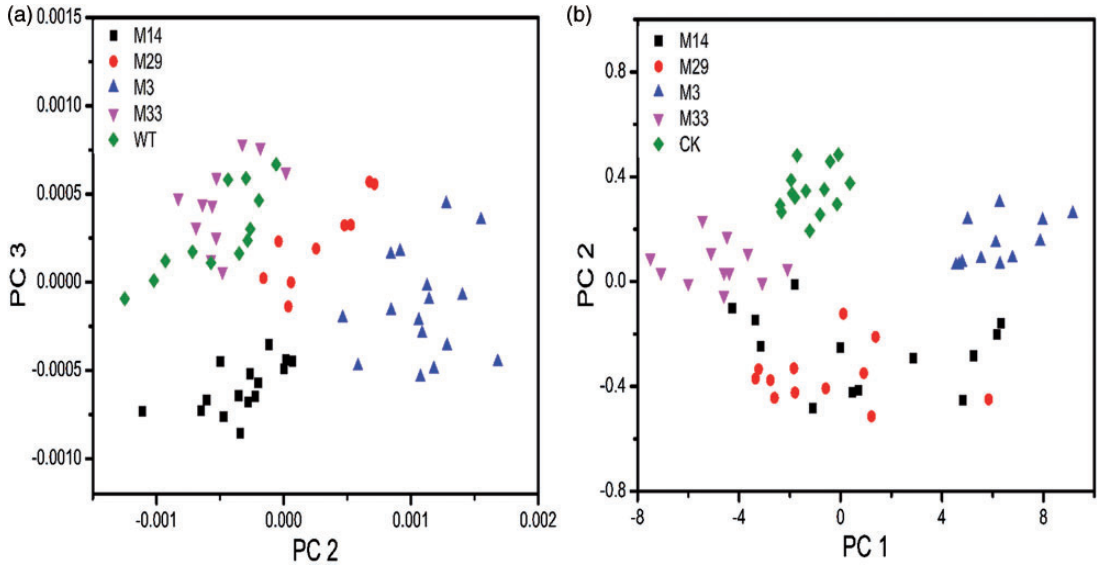

Figure 5. Principal component analysis (PCA) of FT-IR (a) and Raman (b) spectra of astaxanthin-hyperproducing and WT strains.

raw spectra, they can be distinguished by Raman spectra via treatment with the MCR algorithm. In addition, for distinguishing astaxanthin and β-carotene, the assignments of the Raman and FT-IR maps are also corroborated by the respective cellular location of astaxanthin, β-carotene, and lipids in the same *H. pluvialis* cell (see Supplemental Figure 6a online). It can be found that the locations of astaxanthin and β-carotene are different in the Raman maps while the lipid distribution matches very well with the location of astaxanthin in FT-IR maps.

Comparison of astaxanthin, β-carotene, and chlorophyll yields among the different strains showed that the contents of these components in M16, M20, and M29 are comparable with that of the WT strain, while M33 has higher chlorophyll and less astaxanthin than the WT strain. In particular, M3 and M14 have much higher astaxanthin content. The density distribution of carotenoid in different strains revealed by Raman microspectroscopy was consistent with that assessed by FT-IR microspectroscopy. In addition, the time dependence of astaxanthin production during the different stages of cell growth was also recorded. The content of astaxanthin in the M3 mutant was observed to be significantly higher than in the WT strain at the corresponding culture time (see Supplemental Figure 7 online). The contents of β-carotene and chlorophyll decreased with the age of the red cyst cells, which is in agreement with other previous work.[43] The pigment contents of β-carotene and chlorophyll in the M3 mutant were higher compared with the WT strain at the early culture stage, as observed by Raman microspectroscopy. The faster increase in astaxanthin content in the M3 strain is closely related to the high level of β-carotene and chlorophyll because the β-carotene is the precursor of astaxanthin, and it is distributed at the cytoplasmic lipid vesicles and the chloroplasts, which provide the site of the photosynthesis and supply the raw materials for astaxanthin synthesis.[36]

PCA Identification Based on FT-IR and Raman Spectra

As shown in the foregoing sections, FT-IR and Raman microspectroscopy for single-cell inspection is very useful, not only for probing the astaxanthin production in different individual cells at different growth stages, but also for revealing the distribution of multiple components as well as their relationships, such as the relationship between astaxanthin and β-carotene. Nevertheless, it is still necessary to investigate the algal strains by making measurements on multiple cells or the bulk samples for verification. For this purpose, we harvested enough algal cells, recorded their FT-IR and Raman spectra, and analyzed the spectra using a chemometrics approach for strain identification and discrimination.

For the data analysis we employed PCA to differentiate the different strains based upon differences in FT-IR and Raman spectral features of bulk samples. Principal component analysis (PCA) is a common multivariate statistical analysis technique which is widely employed in the interpretation of spectral data variance. The major advantage of PCA is that it reduces a multidimensional data set to its most dominant features, removes the random variation (noise), and retains the principal components (PCs) that capture the related variation. Figure 5 shows the PCA data analysis for the FT-IR spectra in the region 3100–2800 cm^{-1} and for the Raman spectra in the region of 2800–400 cm^{-1}, respectively. Four PCs for FT-IR and three PCs for Raman were used. As can be seen from the score plots in Figure 5a (i.e., PC2 versus PC3 for FT-IR data and PC1 versus PC2 for Raman data; other choices,

e.g., PC1 versus PC2 and PC2 versus PC3 from Raman and FT-IR are also provided in Supplemental Figure 8 online), different strains can be well distinguished, suggesting that the spectral variation is closely associated with the distinctive contents of astaxanthin, β-carotene, and chlorophyll. It should be noted, however, Figure 5 also shows that PCA of FT-IR spectra cannot clearly distinguish M33 from WT strains, while PCA of Raman spectra cannot clearly distinguish M14 from M29 strains, suggesting the limitation to some extent of a single spectroscopic tool in the application. Therefore, we propose that a most effective way of utilization of spectroscopic tools is to combine of both FT-IR and Raman spectroscopy in the application. Actually, IR and Raman spectroscopy are complementary techniques because different selection rules apply for IR absorption and Raman scattering characteristic bands. Combination of both techniques can provide a complete and highly specific vibrational spectroscopic fingerprint of cells.[47]

Finally, we would like to emphasize that our spectroscopic approach may advance the screening time essentially for analyzing and identifying different algal strains with variable accumulation of β-carotene, astaxanthin, proteins, lipids, and carbohydrates. For example, we found that the spectral analysis result of the algal strains cultured under high light stress condition for 20 days is consistent with that for the algal strains for 30 days (see Supplemental Figures 2, 5, and 7 online). This suggests that monitoring single cells with FT-IR and Raman microspectroscopy at an early stage can predict the astaxanthin yield in the later stage, and so we can reduce the screening time significantly.

Conclusion

In summary, we have successfully applied FT-IR and Raman spectroscopy in the effective screening of varied *Haematococcus* strains in this work. We have employed FT-IR and Raman microspectroscopy and an imaging technique to analyze the relative concentrations of chlorophyll, astaxanthin, β-carotene, and other cellular components at the single cell level with spatially resolved visualization of components location in the algal cells. Through FT-IR measurements, we have shown that the ratio of 1740 cm^{-1} band to 1156 cm^{-1} band in the FT-IR spectra can be used to analyze and identify the astaxanthin-hyperproducing mutants. With Raman microspectroscopy and imaging, we have found that it is possible to assess the components, including astaxanthin, β-carotene, and chlorophyll, and their distributions in the algal cells quickly based on the MCR analysis of the spectra.

Moreover, this work also demonstrates that combination of both FT-IR and Raman spectroscopy is very powerful with the aid of multivariate statistical analysis methods such as PCA and MCR in the screening of astaxanthin-hyperproducing algal strains. Especially, with MCR treatment, the high chemical contrast in single cells can be obtained via Raman imaging, which can identify the individual pure components including astaxanthin, β-carotene, and chlorophyll. As for the analysis of bulk samples, the method of PCA shows good ability for distinguishing different algal strains. Our results also indicate that the FT-IR method is better for chemometric analysis while the Raman method is better for chemically based imaging.

Therefore, our research demonstrates the new approach based on spectroscopic techniques to identify astaxanthin-hyperproducing *Haematococcus* strains and, as such, may open a new door for developing quick and convenient screening methods advantageous to the mutants breeding industry.

Acknowledgments

The FT-IR facility was provided by the National Synchrotron Radiation Laboratory (NSRL, China), and we would like to thank Dr. Zeming Qi for his assistance in the FT-IR measurement.

Conflict of Interest

None declared

Funding

This work was financially supported by the National Natural Science Foundation of China (grant number 11475217) and the Strategic Priority Research Program of the Chinese Academy of Sciences (grant number XDA08040107).

Supplemental Material

All supplemental material mentioned in the text, including eight figures, is available in the online version of the journal, at http://asp.sagepub.com/supplemental

References

1. I. Higuera-Ciapara, L. Félix-Valenzuela, F.M. Goycoolea. "Astaxanthin: A Review of Its Chemistry and Applications". Crit. Rev. Food Sci. 2006. 46: 185–196.
2. W. Miki. "Biological Functions and Activities of Animal Carotenoids". Pure Appl. Chem. 1991. 63(1): 141–146.
3. M. Guerin, M.E. Huntley, M. Olaizola. "Haematococcus Astaxanthin: Applications for Human Health and Nutrition". Trends Biotechnol. 2003. 21(5): 210–216.
4. R. Vidhyavathi, L. Venkatachalam, B.S. Kamath, R. Sarada, G.A. Ravishankar. "Differential Expression of Carotenogenic Genes and Associated Changes in Pigment Profile during Regeneration of *Haematococcus pluvialis* Cysts". Appl. Microbiol. Biotechnol. 2007. 75: 879–887.
5. R.T. Lorenz, G.R. Cysewski. "Commercial Potential for Haematococcus Microalgae as a Natural Source of Astaxanthin". Trends Biotechnol. 2000. 18: 160–167.
6. S. Boussiba. "Carotenogenesis in the Green Alga *Haematococcus pluvialis*: Cellular Physiology and Stress Response". Physiol. Plantarum. 2000. 108: 111–117.
7. R. Sarada, U. Tripathi, G.A. Ravishankar. "Influence of Stress on Astaxanthin Production in *Haematococcus pluvialis* Grown under Different Culture Conditions". Process Biochem. 2002. 37: 623–627.

8. P.F. Ip, K.H. Wong, F. Chen. "Enhanced production of astaxanthin by the green microalga Chlorella zofingiensis in mixotrophic culture". Process Biochem. 2004. 39(11): 1761–1766.
9. U. Tripathi, G. Venkateshwaran, R. Sarada, G.A. Ravishankar. "Studies on *Haematococcus pluvialis* for Improved Production of Astaxanthin by Mutagenesis". World. J. Microbiol. Biotechnol. 2001. 17: 143–148.
10. B.S. Kamath, R. Vidhyavathi, R. Sarada, G.A. Ravishankar. "Enhancement of Carotenoids by Mutation and Stress Induced Carotenogenic Genes in *Haematococcus pluvialis* Mutants". Bioresour. Technol. 2008. 99: 8667–8673.
11. Y. Chen, D.F. Li, W.Q. Lu, J.J. Xing, B.D. Hui, Y.S. Han. "Screening and Characterization of Astaxanthin-Hyperproducing Mutants of *Haematococcus pluvialis*". Biotechnol. Lett. 2003. 25: 527–529.
12. N. Chumpolkulwong, T. Kakizono, T. Handa, N. Nishio. "Isolation and Characterization of Compactin Resistant Mutants of an Astaxanthin Synthesizing Green Alga *Haematococcus pluvialis*". Biotechnol. Lett. 1997. 19(3): 299–302.
13. G. Bonente, C. formighieri, M. Mantelli, C. Catalanotti, G. Giuliano, T. Morosinotto, R. Bassi. "Mutagenesis and Phenotypic Selection as a Strategy Toward Domestication of *Chlamydomonas reinhardtii* Strains for Improved Performance in Photobioreactors". Photosynth. Res. 2011. 108: 107–120.
14. D. Naumann, D. Helm, H. Labischinski. "Microbiological Characterizations by FT-IR Spectroscopy". Nature. 1991. 351: 81–82.
15. R.J.L. Meanwell, G. Shama. "Direct FTIR Assay of Streptomycin in Agar". Biotechnol. Lett. 2005. 27: 1629–1631.
16. B.Y. Li, N.M.S. Sirimuthu, B.H. Ray, A.G. Ryder. "Using Surface-Enhanced Raman Scattering (SERS) and Fluorescence Spectroscopy for Screening Yeast Extracts, a Complex Component of Cell Culture Media". J. Raman Spectrosc. 2012. 43: 1074–1082.
17. I. Sayin, M. Kahraman, F. Sahin, D. Yurdakul, M. Culha. "Characterization of Yeast Species Using Surface-Enhanced Raman Scattering". Appl. Spectrosc. 2009. 63(11): 1276–1282.
18. D. Helm, D. Naumann. "Identification of Some Bacterial-Cell Components by FT-IR Spectroscopy". FEMS Microbiol. Lett. 1995. 126: 75–79.
19. A. Szeghalmi, S. Kaminskyj, K.M. Gough. "A Synchrotron FTIR Microspectroscopy Investigation of Fungal Hyphae Grown Under Optimal and Stressed Conditions". Anal. Bioanal. Chem. 2007. 387: 1779–1789.
20. K. Jilkine, K.M. Gough, R. Julian, S.G.W. Kaminskyj. "A Sensitive Method for Examining Whole-Cell Biochemical Composition in Single Cells of Filamentous Fungi Using Synchrotron FTIR Spectromicroscopy". J. Inorg. Biochem. 2008. 102: 540–546.
21. Y.S. Huang, T. Karashima, M. Yamamoto, H. Hamaguchi. "Molecular-Level Investigation of the Structure, Transformation, and Bioactivity of Single Living Fission Yeast Cells by Time- and Space-Resolved Raman Spectroscopy". Biochemistry. 2005. 44: 10009–10019.
22. Y. Naito, A. Toh-E, H. Hamaguchi. "In Vivo Time-Resolved Raman Imaging of A Spontaneous Death Process of A Single Budding Yeast Cell". J. Raman Spectrosc. 2005. 36: 837–839.
23. C.K. Huang, H. Hamaguchi, S. Shigeto. "In Vivo Multimode Raman Imaging Reveals Concerted Molecular Composition and Distribution Changes During Yeast Cell Cycle". Chem. Commun. 2011. 47: 9423–9425.
24. M. Okuno, H. Kano, P. Leproux, V. Couderc, J.P.R. Day, M. Bonn, H. Hamaguchi. "Quantitative CARS Molecular Fingerprinting of Single Living Cells with the Use of the Maximum Entropy Method". Angew. Chem. Int. Edit. 2010. 49: 6773–6777.
25. X.N. He, J. Allen, P.N. Black, T. Baldacchini, X. Huang, H. Huang, L. Jiang, Y.F. Lu. "Coherent Anti-Stokes Raman Scattering and Spontaneous Raman Spectroscopy and Microscopy of Microalgae with Nitrogen Depletion". Biomed. Opt. Express. 2012. 3: 2896–2906.
26. A. Dementjev, J. Kostkevičlene. "Applying the Method of Coherent Anti-Stokes Raman Microscopy for Imaging of Carotenoids in Microalgae and Cyanobacteria". J. Raman Spectrosc. 2013. 44: 973–979.
27. A.M. Barlow, A.D. Slepkov, A.R. Ridsdale, P.J. Mcginn, A. Stolow. "Label-Free Hyperspectral Nonlinear Optical Microscopy of the Biofuel Micro-Algae *Haematococcus pluvialis*". Biomed. Opt. Express. 2014. 5: 3391–3402.
28. U. Tripathi, R. Sarada, R.S. Rao, G.A. Ravishankar. "Production of Astaxanthin in *Haematococcus pluvialis* Cultured in Various Media". Bioresour. Technol. 1999. 68: 197–199.
29. M. Kobayashi, T. Kakizono, N. Nishio, S. Nagai, Y. Kurimura, Y. Tsuji. "Antioxidant Role of Astaxanthin in the Green Alga *Haematococcus pluvialis*". Appl. Microbiol. Biotechnol. 1997. 48(3): 351–356.
30. B.H. Davies. "Carotenoids". In: T.W. Goodwin (ed.) Chemistry and Biochemistry of Plant Pigments. Vol. 2, London, UK: Academic Press, 1976, pp.38–166.
31. S. Boussiba, A. Vonshak. "Astaxanthin Accumulation in the Green Alga *Haematococcus pluvialis*: Effects of Cultivation Parameters". Plant Cell Physiol. 1991. 32(7): 1077–1082.
32. H.D.T. Jones, D.M. Haaland, M.B. Sinclair, D.K. Melgaard, M.H. Van Benthem, M.C. Pedroso. "Weighting Hyperspectral Image Data for Improved Multivariate Curve Resolution Results". J. Chemometr. 2008. 22: 482–490.
33. D.M. Haaland, H.D.T. Jones, M.H. Van Benthem, M.B. Sinclair, D.K. Melgaard, C.L. Stork, M.C. Pedroso, P. Liu, A.R. Brasier, N.L. Andrews, D.S. Lidke. "Hyperspectral Confocal Fluorescence Imaging: Exploring Alternative Multivariate Curve Resolution Approaches". Appl. Spectrosc. 2009. 63(3): 271–279.
34. A.M. Collins, H.D.T. Jones, D.X. Han, Q. Hu, T.E. Beechem, J.A. Timlin. "Carotenoid Distribution in Living Cells of Haematococcus Pluvialis (Chlorophyceae)". PLoS One. 2011. 6(9): 1–7.
35. R. Vidhyavathi, L. Venkatachalam, R. Sarada, G.A. Ravishankar. "Regulation of Carotenoid Biosynthetic Genes Expression and Carotenoid Accumulation in the Green Alga Haematococcus Pluvialis under Nutrient Stress Conditions". J. Exp. Bot. 2008. 59(6): 1409–1418.
36. K. Grunewald, J. Hirschberg, C. Hagen. "Ketocarotenoid Biosynthesis Outside of Plastids in the Unicellular Green Alga *Haematococcus pluvialis*". J. Biol. Chem. 2001. 276(8): 6023–6029.
37. S.B. Wang, F. Chen, M. Sommerfeld, Q. Hu. "Isolation and Proteomic Analysis of Cell Wall-Deficient *Haematococcus pluvialis* Mutants". Proteomics. 2005. 5: 4839–4851.
38. M.H. Moh, Y.B.C. Man, B.S. Badlishah, S. Jinap, M.S. Saad, W.J.W. Abdullah. "Quantitative Analysis of Palm Carotene Using Fourier Transform Infrared and Near Infrared Spectroscopy". J. Am. Oil Chem. Soc. 1999. 76(2): 249–254.
39. P.A. Tarantilis, A. Beljebbar, M. Manfait, M. Polissiou. "FT-IR, FT-Raman Spectroscopic Study of Carotenoids from Saffron (*Crocus sativus* L.) and Some Derivatives". Spectrochim. Acta, Part A. 1998. 54: 651–657.
40. M. KačUrákováa, P. Capeka, V. Sasinkováa, N. Wellnerb, A. Ebringerová. "FT-IR Study of Plant Cell Wall Model Compounds: Pectic Polysaccharides and Hemicelluloses". Carbohydr. Polym. 2000. 43: 195–203.
41. R.T. Lorenz. "A Technical Review of Haematococcus Algae" Naturose™ Technical Bulletin #060. Kailua-Kona, HI: Cyanotech Corporation. 1999. 1–12.
42. M. Zhekisheva, S. Boussiba, I. Khozin-Goldberg, A. Zarka, Z. Cohen. "Accumulation of Oleic Acid in *Haematococcus pluvialis* (Chlorophyceae) Under Nitrogen Starvation or High Light is Correlated with That of Astaxanthin Esters". J. Phycol. 2002. 38(2): 325–331.
43. S. Tan, F.X. Cunningham, M. Youmans, B. Grabowski, Z. Sun, E. Gantt. "Cytochrome F Loss in Astaxanthin Accumulating Red Cells of *Haematococcus pluvialis* (Chlorophyceae): Comparison of Photosynthetic Activity, Photosynthetic Enzymes and Thylakoid Membrane Polypeptides in Red and Green Cells". J. Phycol. 1995. 31: 897–905.

44. A. Kaczor, K. Turnau, M. Baranska. "In Situ Raman Imaging of Astaxanthin in a Single Microalgal Cell". Analyst. 2011. 136(6): 1109–1122.
45. D. Zhang, P. Wang, M.N. Slipchenko, D. Ben-Amotz, A.M. Weiner, J.X. Cheng. "Quantitative Vibrational Imaging by Hyperspectral Stimulated Raman Scattering Microscopy and Multivariate Curve Resolution Analysis". Anal. Chem. 2013. 85(1): 98–106.
46. B.O. Budevsk, S.T. Sum, T.J. Jones. "Application of Multivariate Curve Resolution for Analysis of FT-IR Microspectroscopic Images of In Situ Plant Tissue". Appl. Spectrosc. 2003. 57(2): 124–131.
47. K. Maquelin, C. Kirschner, L.-P. Choo-Smith, N. Van Den Braak, H. Ph. Endtz, D. Naumann, G.J. Puppels. "Identification of Medically Relevant Microorganisms by Vibrational Spectroscopy". J. Microbiol. Methods. 2002. 51: 255–271.